IJCRT.ORG ISSN : 2320-2882

INTERNATIONAL JOURNAL OF CREATIVE RESEARCH THOUGHTS (IJCRT)

An International Open Access, Peer-reviewed, Refereed Journal

ASSESSMENTS OF EXACT AND ASSUMED THROUGH THICKNESS TEMPERATURE DISTRIBUTION FOR EXPONENTIALLY VARIED FG LAMINATE

[1]Sandeep S. Pendhari and [2]Sharawari P. Kulkarni

[1] Associate Professor, [2] Research Scholar

[1]Structural Engineering Department, Veermata Jijabai Technological Institute, Matunga, Mumbai 400 019, India

Abstract: This paper describes an analytical solution for solving the heat conduction equation, which determines the exact temperature profile along with the thickness of the simply supported laminate. The further exponential varied thermal field has considered, and comparison with exact variation has carried out to suggest remarkable output in this area. Heat conductivity, modulus of elasticity, and coefficient of thermal expansion have graded exponentially in the thickness direction of laminates. An in-depth study in this area further leads to a concrete solution for stress analysis

Index Terms: FG Laminate, Semi-analytical, Exact, Heat conduction, Exponential

I . INTRODUCTION

Functionally graded materials (FGMs) have developed first in Japan in 1984 to cater to the requirement of enormous temperature difference through a width of 10mm or so. In FGM, material variation has considered along with one or multiple directions of laminates. These gradations in materials discussed along with power law or with exponential law give the best benefits of different single elemental materials. Composite materials delamination problems can overcome by considering the smooth, gradual, and continuous variation of material properties and volume fractions of ingredients.

Generally, FGM has used in a thermal environment. Depend on the Euler-Bernoulli theory (EBT), Sankar [1] published an elasticity solution for simply supported functionally graded (FG) beams only for sinusoidal loading. Here they have assumed an exponential variation of elastic constants and temperature. FG material is a combination of two elements, generally ceramic and metal. To decide its composition under steady temperature and thermal shock and its effect on crack propagation related study have carried out by Noda [2]. Giunta et al. [3][4] have used an actual temperature pattern by using a heat conduction equation with unified formulation to study thermal stresses in monolayer and sandwich cross-section FG beam. Here, Giunta has also carried out a similar study by using Wendland's radial basis function for Isotropic and laminated orthotropic beam. Pietro et al. [5] also used a temperature profile as per the heat conduction equation. They used a unified formulation with the finite element method to study the FG beam with linear, quadratic, and cubic material gradation. The buckling behavior of the FG beam has reviewed by Kiani and Eslami [6]. They have considered uniform, linear, and nonlinear temperature variation with power law material gradation.

By examining the similar kind of temperatures, Trinh et al. [7] derived an exact solution by state space approach to study buckling and vibration of the Functionally graded beam. EI-Ashmawy et al. [8] invented a finite element model based on the Timoshenko approach to observe the difference in the dynamic response of axially and transversally loaded FGB. Static analysis has carried out many of the researchers, Chakraborty et al. [9] developed a new beam element based on first-order shear deformation theory. To determine the location of neutral surface, Kadoli et al. [10] used higher-order shear deformation theory. The behavior of short FG beam under three-point bending has studied by Benatta et al. [11] by assuming power law variation of material along with the depth of the beam. Generally, material variation has considered as per either exponential law or as per power law. However, in both power-law and exponential functions, the stress concentrations appear in one of the interfaces in which the material is continuous with rapid change. To avoid this, Sallai et al. [12] have study stress intensity of cracked body by considering both variations together called sigmoid. Comparative studies between the number of shear deformation theories have been performed by Thai and Vo [13] to investigate the effect of the power-law index on the bending and free vibration responses of the FG beam. Influence of material length scale parameter, different material compositions, and shear deformation modes on static and free vibration analyses of FG micro-beam have investigated by Simsek and Reddy [14] by adopting a size-dependent unified beam theory. Here, Simsek and Reddy also studied the buckling behavior of functionally graded microbeam embedded in an elastic medium using the modified couple stress theory. Pendhari et al. [15] presented semi-analytical bending solutions for FG narrow beam subjected to transverse loads.

In this paper, an attempt has taken to generate a semi-analytical formulation by using Fourier's formulation and partial differential equation (PDE) of heat conduction for accurate assessment of temperature field through the depth of FG laminate. Additionally, accurate temperature profile and exponentially considered temperature fields have compared for various materials and different reference temperature ranges. From numerical studies, a remarkable conclusion is obtained and presented here. Developed mathematical models contain the formation of a two-point Boundary Value Problem governed by a group of coupled first-order Ordinary Differential Equations (Eqn. 1) within the depth of the laminate.

$$A(x_3)x_2(x_3) + p(x_3) = \frac{d}{dz}x_2(x_3) \tag{1}$$

Here $y(x_3)$ is an *n*-dimensional vector of primary variables. Number (*n*) equals the order of PDE. For heat conduction formulation, '*n*' is equal to two. $A(x_3)_{(n,n)}$ It is a coefficient matrix (a function of material properties in the thickness direction) and $p(x_3)$ is an *n*-dimensional vector of non-homogenous (loading). It has to note down that loading terms include only body loads such as inertia loads, thermal loads, electric loads, etc. In contrast, surface loads have incorporated into the formulation in the form of boundary conditions during the solution procedure.

II MATHEMATICAL FORMULATIONS

Consider a simply supported single layer FG laminate of thickness '*h*,' length '*a*' in x_1 direction, and width '*b*' in x_2 direction and subjected to thermal loading only as shown in Fig. 1. Hook's law constant (E), thermal expansion coefficient (α) and coefficient of thermal conductivity (λ) have varied only through the thickness of laminate accordingly to exponential law as,

$$E(x_3) = E_0 e^{-In\left(\frac{E_0}{E_t}\right)x_3} \qquad \alpha(x_3) = \alpha_0 e^{-In\left(\frac{\alpha_0}{\alpha_t}\right)x_3} \qquad \lambda(x_3) = \lambda_0 e^{-In\left(\frac{\lambda_0}{\lambda_t}\right)x_3} \tag{2}$$

Here, subscript *0* and *t* defined the respective material properties at the downside of the surface and upper side of the surface of laminates, respectively. Next, it has considered that the FG material is isotropic at every point, and Poisson's ratio has considered being constant throughout the domain. It has to note that Kantrovich and Krylov [16] approach used in present formulations to transfer ruling partial differential equation (PDE) to a group of coupled first-order ordinary differential equations (ODEs)

2.1 Semi-Analytical Heat Conduction Formulation

The use of FG materials is primarily in situations where large temperature fields have experienced on the structure, and hence, accurate determination of structural responses is of the utmost importance. In this section, the closed-form formulation for the heat conduction equation has discussed. A thermal load as defined in Eqn. (3) is assumed with only known temperature value at the upside and bottom side of the laminate surface

$\left(T = T_0 \text{ at } x_3 = 0 \text{ and } T = T_t \text{ at } x_3 = h\right)$.

$$T(x_1, x_2, x_3) = \sum_{m=1}^{\infty} T(x_3)\sin\frac{m\pi x_1}{a}\sin\frac{n\pi x_2}{b} \text{ and } q_z(x_1, x_2, x_3) = \sum_{m=1}^{\infty} q_z(x_3)\sin\frac{m\pi x_1}{a}\sin\frac{n\pi x_2}{b} \tag{3}$$

A governing steady-state heat conduction equation without internal heat generation is,

$$\lambda(x_3)\frac{\partial^2 T(x_1, x_2, x_3)}{\partial x^2} + \lambda(x_3)\frac{\partial^2 T(x_1, x_2, x_3)}{\partial {x_2}^2} + \lambda(x_3)\frac{\partial^2 T(x_1, x_2, x_3)}{\partial {x_3}^2} = 0 \tag{4}$$

As per Fourier's expression of heat conduction, heat flux in direction x_1, x_2 and x_3 has expressed as,

$$\begin{aligned} q_{x_1}(x_1, x_2, x_3) &= -\lambda(x_3)\frac{\partial T(x_1, x_2, x_3)}{\partial x} \\ q_{x_2}(x_1, x_2, x_3) &= -\lambda(x_3)\frac{\partial T(x_1, x_2, x_3)}{\partial x_2} \\ q_{x_3}(x_1, x_2, x_3) &= -\lambda(x_3)\frac{\partial T(x_1, x_2, x_3)}{\partial x_3} \end{aligned} \tag{5}$$

where, q_i = heat flux along x_1, x_2 and x_3-axes (i = x_1, x_2, and x_3) in Wm^{-2}

And, by the consideration, that total of heat remains in the element due to heat flow is zero, the balancing Equation in 3D,

$$\frac{\partial q_{x_1}(x_1, x_2, x_3)}{\partial x_1} + \frac{\partial q_{x_2}(x_1, x_2, x_3)}{\partial x_2} + \frac{\partial q_{x_3}(x_1, x_2, x_3)}{\partial x_3} = 0 \tag{6}$$

Now, two variables viz. heat flux (q_{x_3}) and temperature field (T) are assumed as a primary variable. By using a mathematical simplification of the Eqns. (5) and (6) a group of PDEs consist of only two primary variables T and q_{x_3} are gain, as shown below.

$$\frac{\partial T(x_1, x_3)}{\partial x_3} = -\frac{1}{\lambda(x_3)}q_{x_3}(x_1, x_3) \; ; \; \frac{\partial q_{x_3}(x_1, x_3)}{\partial x_3} = \lambda(x_3)\left[\frac{\partial^2 T(x_1, x_3)}{\partial {x_1}^2} + \frac{\partial^2 T(x_1, x_3)}{\partial {x_2}^2}\right] \tag{7}$$

Substituting Eqn. (3) and it's differential coefficient into Eqn. (7). The underline set of first-order ODE's has achieved.

$$\frac{dT_m(x_3)}{dx_3} = \frac{-1}{\lambda(x_3)} q_{x_3 m}(x_3) \;;\; \frac{dq_{x_3 m}(x_3)}{dx_3} = -\lambda(x_3)\left[\frac{m^2\pi^2}{a^2} + \frac{n^2\pi^2}{b^2}\right] T_m(x_3) \tag{8}$$

The above Equation (8) is valid for the three-dimensional domain. By proper eliminating the dimension, Equation (8) can be reduced to the two-dimensional field as,

$$\frac{dT_m(x_3)}{dx_3} = \frac{-1}{\lambda(x_3)} q_{x_3 m}(x_3); \frac{dq_{x_3 m}(x_3)}{dx_3} = -\lambda(x_3)\frac{m^2\pi^2}{a^2} T_m(x_3) \tag{9}$$

Eqns. (8) and (9) shows the ruling two-point Boundary Value Problem in ODE's in the domain $0 \le x_3 \le h$ with known temperatures at the upper side and the lower side surface of a laminate. The solution of Eq. (8) consists of the conversion of initial value problems (IVPs) from known boundary value problems (BVP), which has tabulated in Table 1. The Fourth-order Runge-Kutta algorithm is used here for numerical integration. Eqns. (8) and (9) shows the ruling two-point Boundary Value Problem in ODE's in the domain $0 \le x_3 \le h$ with known temperatures at the upper side and the lower side surface of a laminate. The solution of Eq. (8) consists of the conversion of initial value problems (IVPs) from known boundary value problems (BVP), which has tabulated in Table 1. The Fourth-order Runge-Kutta algorithm is used here for numerical integration.

III NUMERICAL STUDIES

Computer codes have generated by inserting the developed formulation to find out the exact temperature change through the depth of the FG structure. For the numerical investigation, four material sets have considered, which are commonly used in industry and tabulated in Table 2. Reference temperature at the down surface and the upper surface of laminate have regarded as,

a) $T_0 = 20^0 C$ and $T_t = 100^0 C$ - termed as T_1

b) $T_0 = 20^0 C$ and $T_t = 200^0 C$ - termed as T_2

c) $T_0 = 20^0 C$ and $T_t = 300^0 C$ - termed as T_3

d) $T_0 = 20^0 C$ and $T_t = 1000^0 C$ - termed as T_4 (10)

e) $T_0 = 275^0 C$ and $T_t = 1000^0 C$ - termed as T_5

f) $T_0 = 300^0 C$ and $T_t = 1000^0 C$ - termed as T_6

Based on the convergence studies (not presented here for the sake of brevity), around 20 to 30 steps have used through the thickness of laminate for numerical integration. Distribution of temperature field along the thickness of FG laminate for all material sets have obtained by developed formulation for side to thickness ratio (s) 5, 10, 20, and 50 for 2D as well as for 3D. Square and or Rectangular plates for various in-plane aspect ratio $\left(b/a = 1.0, 1.5,\ 2.0,\ 2.5 \text{ and } 3.0\right)$ has considered for numerical investigations. Similarly, the exponential temperature distribution for reference temperatures has obtained. Both these variations have plotted in Fig. 2 to 5 for the FG beam and in Fig. 6 to 9 for the FG plate.

From all figures, it has observed that the difference between exact temperature variation and exponential temperature variation is dependent on material properties, reference temperature, and heat flux at the downside of the surface and upper side of the surface of the laminate. However, no impact of aspect ratios $\left(a/h\right)$ as well in-plane aspect ratios $\left(b/a\right)$ have noticed. When the percentage difference between the heat flux of FG materials is more than the percentage difference between reference temperature, the exponential temperature profile underestimates the exact temperature profile and vice versa. Overestimation of exact temperature over the exponential temperature profile observed from Fig. 2 for material set 1. Here, the percentage difference between top and bottom surface heat flux is more than all reference temperatures, whereas, from Fig. 5, precisely opposite behavior has noticed as this relation is different for material set 4. Further, it has also seen that when the percentage difference between the heat flux of FG materials equal to the percentage difference between reference temperature, exact temperature profile coincides with the assumed exponential temperature profile. It has also been noting down from Fig. 1d, 2c, 3c, and 4a, 4e, 4f, respectively.

IV CONCLUSION

In this produced study, exact temperature distribution through the depth of FG laminate with a semi-analytical approach has derived. Further, its comparison with the exponential temperature profile has carried out. For achieving the real relationship between exact and exponential temperature profile, various material sets and a wide range of reference temperatures considered. It has observed that material properties influence this relationship. Effect of aspect ratio from thin to thick laminate has not seen; simultaneously, the impact of in-plane aspect ratio has also not observed on heat-conduction solutions. Based on this study, when the difference between heat flux and reference temperature are close to each other, judgment can be made to direct the use of an exponential temperature profile instead of finding an accurate temperature profile for thermal stress analysis.

REFERENCES

[1] Sankar B.V. and Tzeng J. T, Thermal stresses in functionally graded beams, *AIAA Journal*, (2002), 40(06), 1228-12232.

[2] Noda N. Thermal Stresses in Functionally Graded Materials. *Journal of Thermal Stresses*, (1999), 22, 477-512.

[3] Giunta G., Metla N., Belouettar S., Ferreira A.J.M., and Carrera E, Thermo-Mechanical Analysis of Isotropic and Composite Beams via Collocation with Radial Basis Functions, *Journal of Thermal Stresses* (2013),36(11),1169-1199.

[4] Giunta G, Crisafulli D. Belouettar S and Carrera E, A thermo-mechanical analysis of functionally graded beams via hierarchical modeling, *Composite Structures*, (2013), 95, 676-690.

[5] Pietro G.D, Hui Y., Giunta G., Belouettar S., Carrera E. and Hu H, A Thermal stress finite element analysis of beam structures by hierarchical modeling." *Composites Part B*, .(2016), 95, 179-195.

[6] Kiani Y. and Eslami M.R, Thermal buckling analysis of functionally graded material beams. *International Journal of Mechanics and Materials in Design*, (2010), 6, 229–238.

[7] Trinh L.C., Vo T.P., Thai H.T. and Nguyen T.K An analytical method for the vibration and buckling of functionally graded beams under mechanical and thermal load, *Composites Part B*,(2016), 100, 152-163.

[8] El-Ashmawy A.M., Kamel M.A., and Elshafei M.A, Thermo-mechanical analysis of axially and transversally Function Graded Beam, *Composites Part B*, (2016),102, 134-149.

[9] Chakraborty A., Gopalakrishnan S. and Reddy J.N, A new beam finite element for the analysis of functionally graded materials, *International Journal of Mechanical Sciences*, (2003),45, 519-539.

[10] Kadoli R., Akthar K, and Ganesan N, Static analysis of functionally graded beams using higher-order shear deformation theory, *Applied Mathematical Modelling*, (2008),38, 2509-2525.

[11] Benatta M.A., Mechab I., Tounsi A, and Adda Bedia E.A, Static analysis of functionally graded short beams including warping and shear deformation effects, *Computational Materials Science*, (2008), 44, 765-773.

[12] Sallai B.O, Abedlouadhed T., Ismail M., Mohamed B.B., Mustapha M., and El Abbas A.B, A theoretical analysis of flexional bending of Al/Al2O3 S-FGM thick beams, *Computational Materials Science*, (2009), 44, 1344-1350.

[13] Thai H.T. and Vo T.P, Bending and free vibration of functionally graded beams using various higher-order shear deformation beam theories, *International Journal of Mechanical Sciences*, (2012), 62, 57–66.

[14] Şimşek M. and Reddy J.N, Bending and vibration of functionally graded microbeams using a new higher-order beam theory and the modified couple stress theory, *International Journal of Engineering Science*, (2013),64, 37 – 53.

[15] Pendhari S.S., Kant T., Desai Y.M. and Subbaiah C.V. On deformation of functionally graded narrow beams under transverse loads, *International Journal of Mechanics and Materials in Design*, (2010), 6, 269 – 282.

[16] Kantrovich L. V. and Krylov V. I, Approximate Methods of Higher Analysis, 3rd Edition, Noordhoff, Groningen, (1958) 304-327.

[17] Ying Ji, Lu C.F. and LIM C.W, 3D thermoelasticity solutions for functionally graded thick plates, *Journal of Zhejiang University SCIENCE A 3*, (2009),10, 327-336

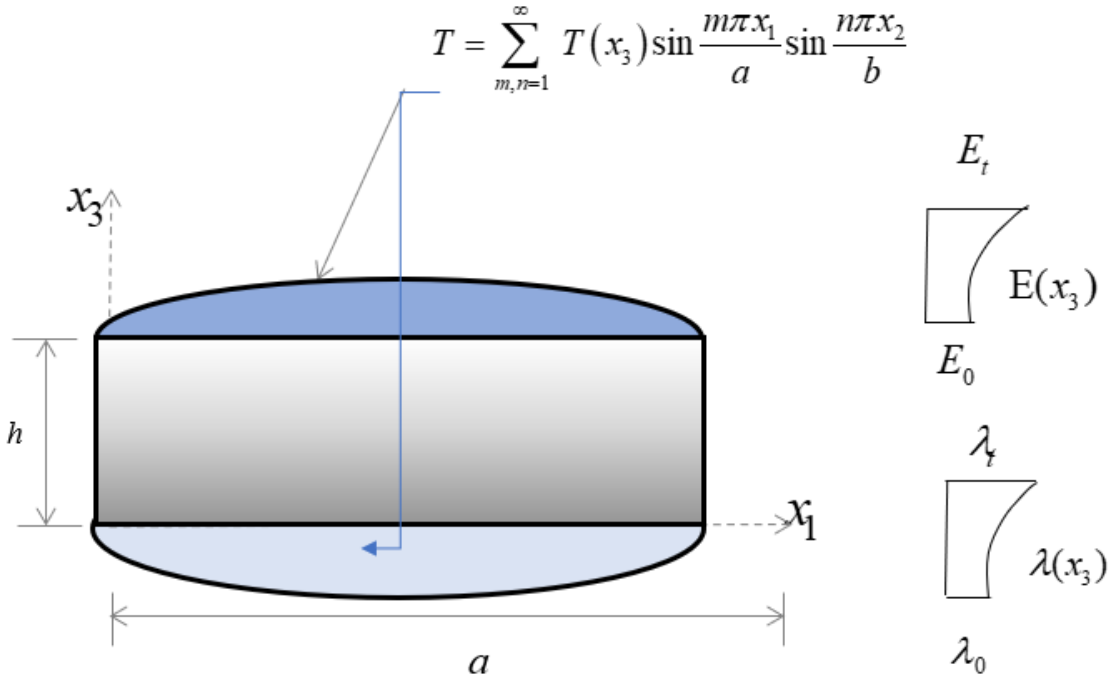

Figure 1. FG laminate subjected to thermal loading

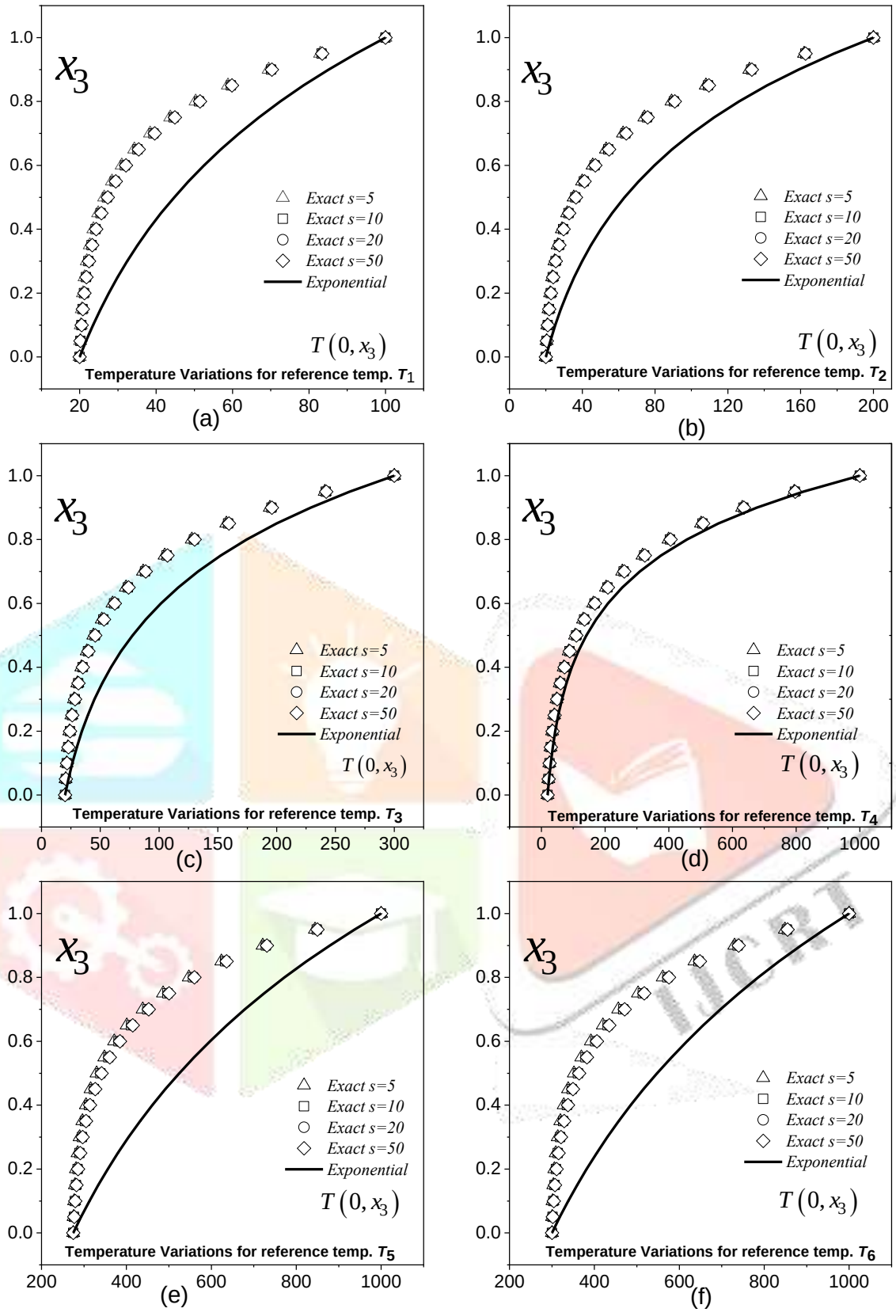

Fig. 2. Comparison of exact and exponential through thickness temperature variation for various aspect ratios $\left(s = a/h\right)$ for FG beam (Material set 1)

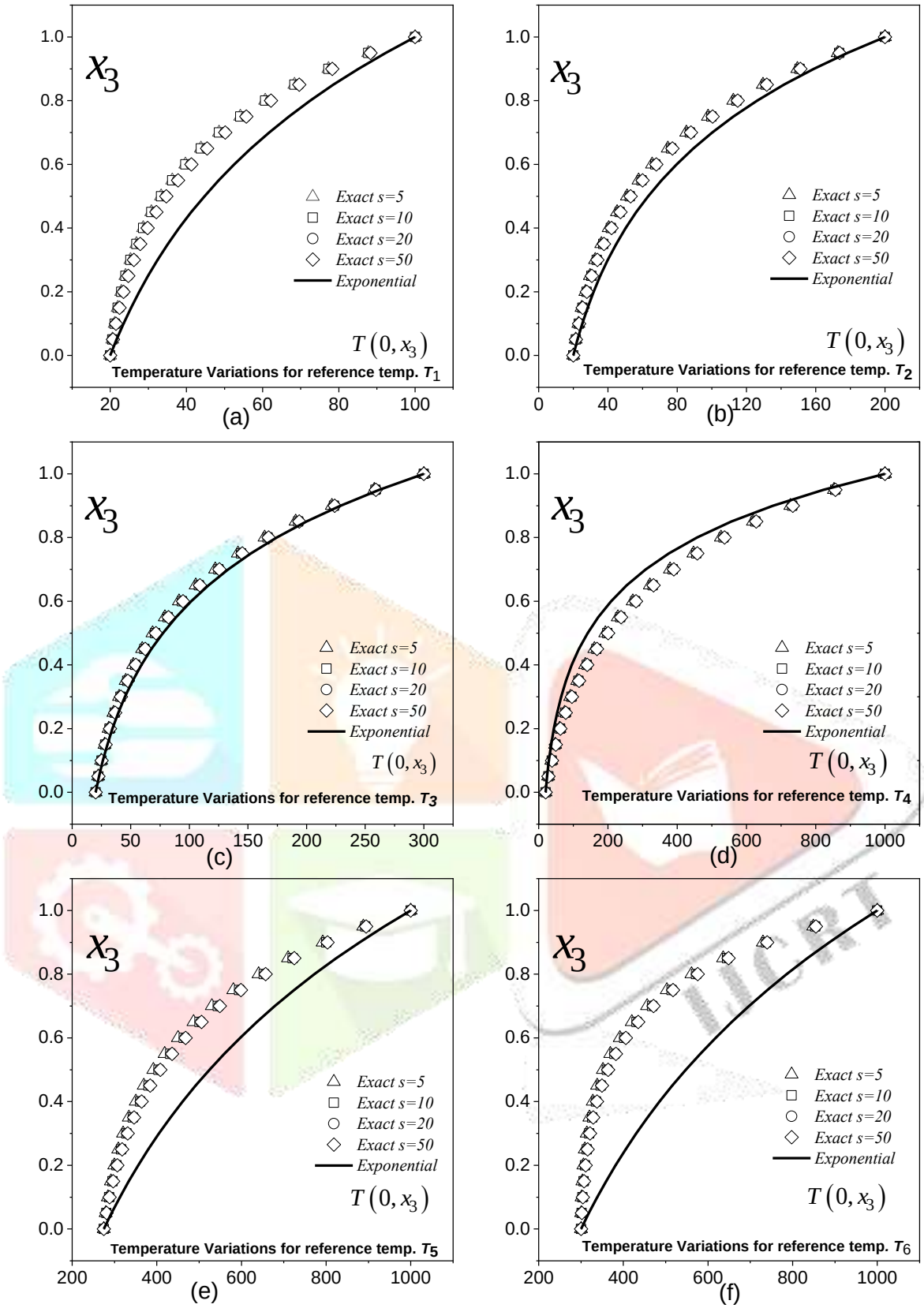

Fig. 3. Comparison of exact and exponential through thickness temperature variation for various aspect ratios $\left(s = a/h\right)$ for FG beam (Material set 2)

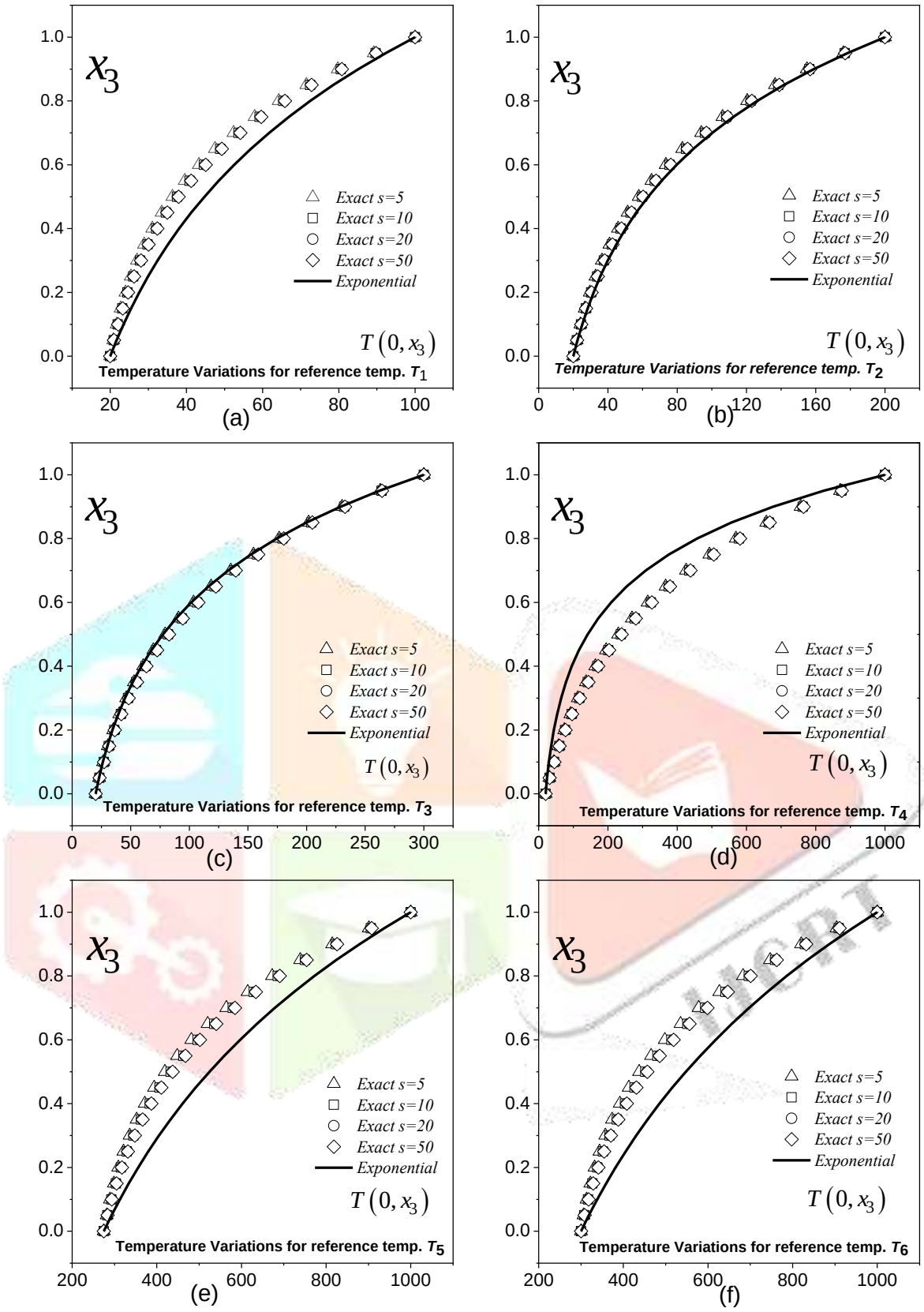

Fig. 4. Comparison of exact and exponential through thickness temperature variation for various aspect ratios $\left(s = a/h\right)$ for FG beam (Material set 3)

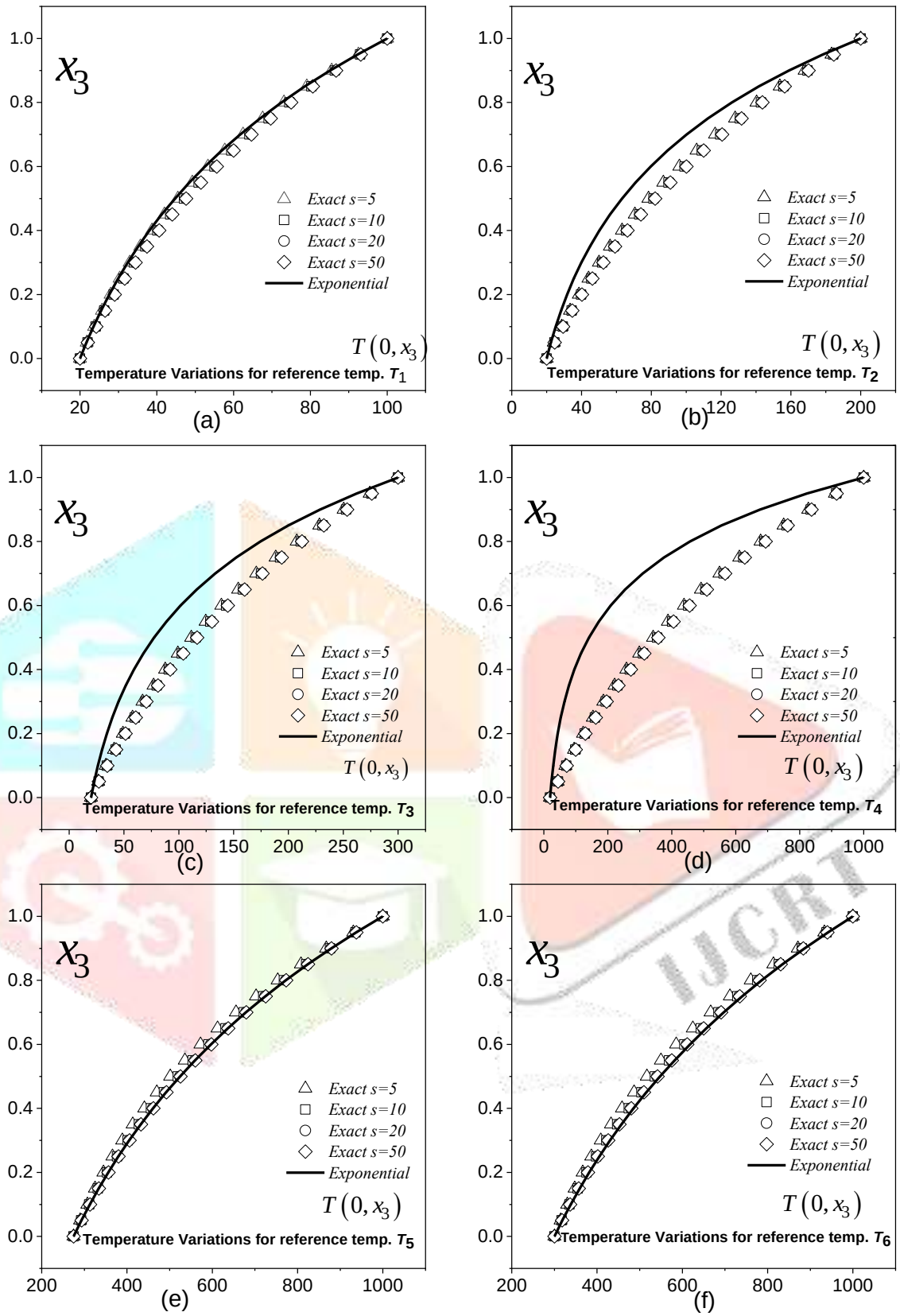

Fig. 5. Comparison of exact and exponential through thickness temperature variation for various aspect ratios $\left(s = a/h\right)$ for FG beam (Material set 4)

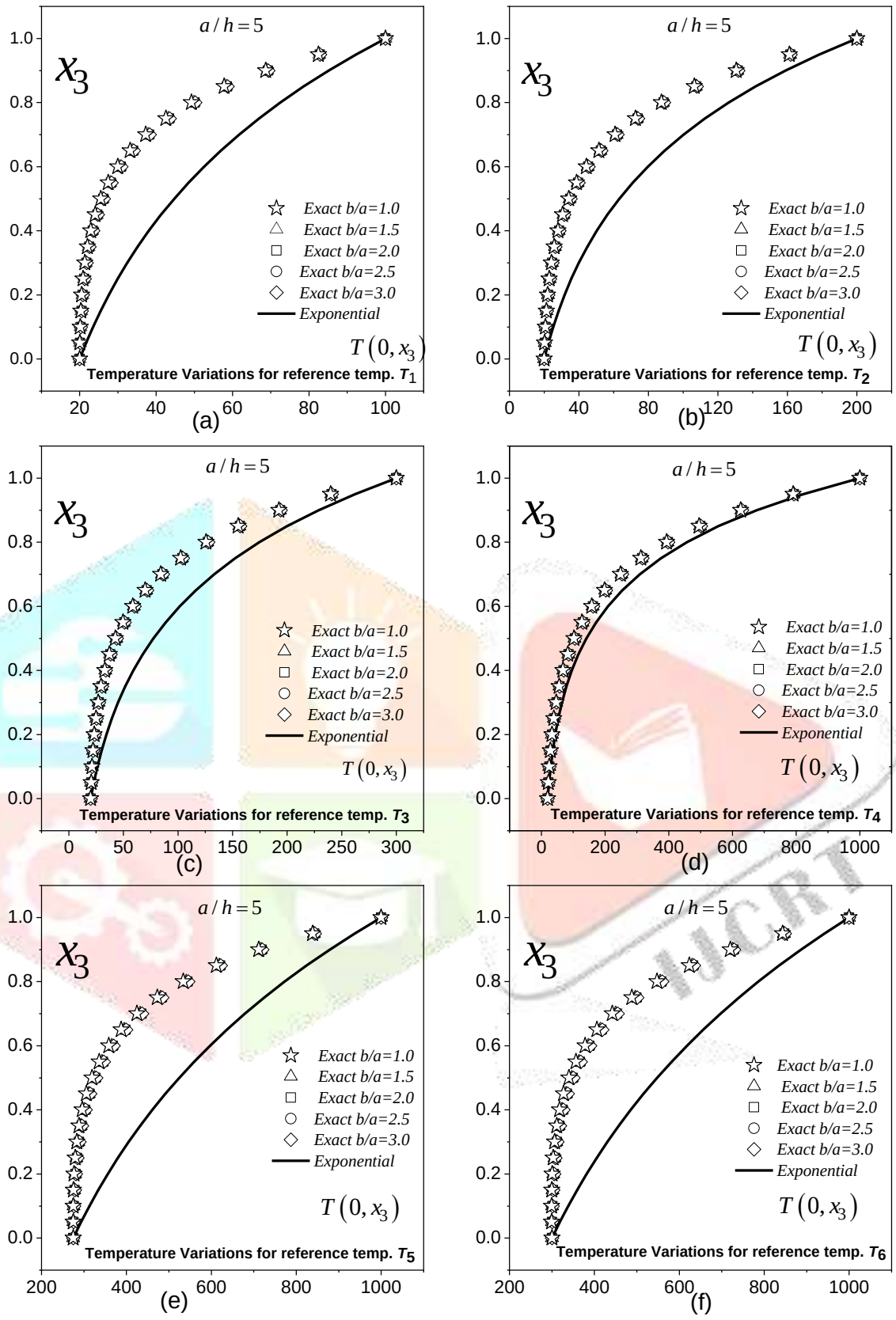

Fig. 6. Comparison of exact and exponential through thickness variation for various in-plane aspect ratios $\left(b/a\right)$ for FG plate (Material set 1)

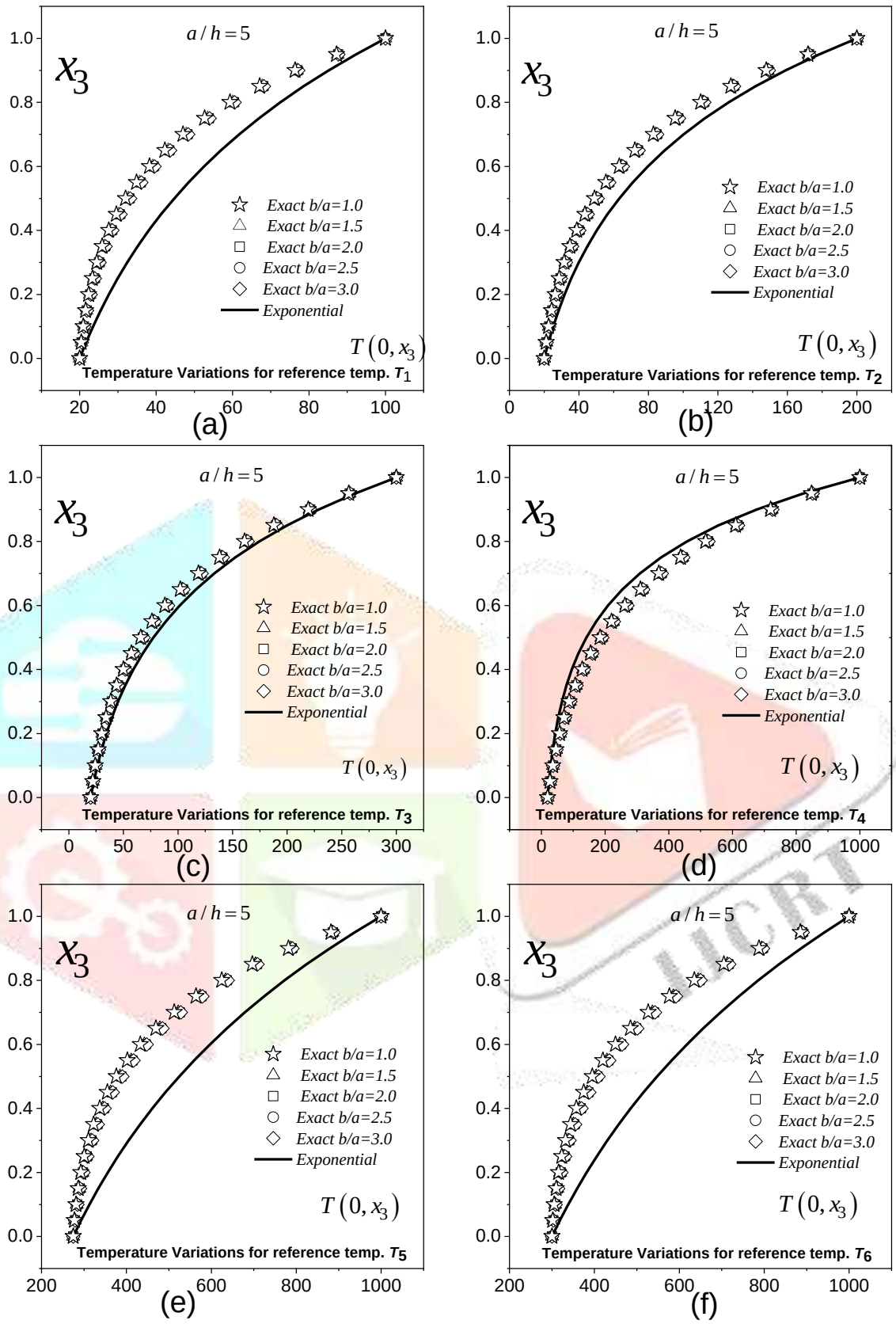

Fig. 7. Comparison of exact and exponential through thickness variation for various in-plane aspect ratios $\left(b/a\right)$ for FG plate (Material set 2)

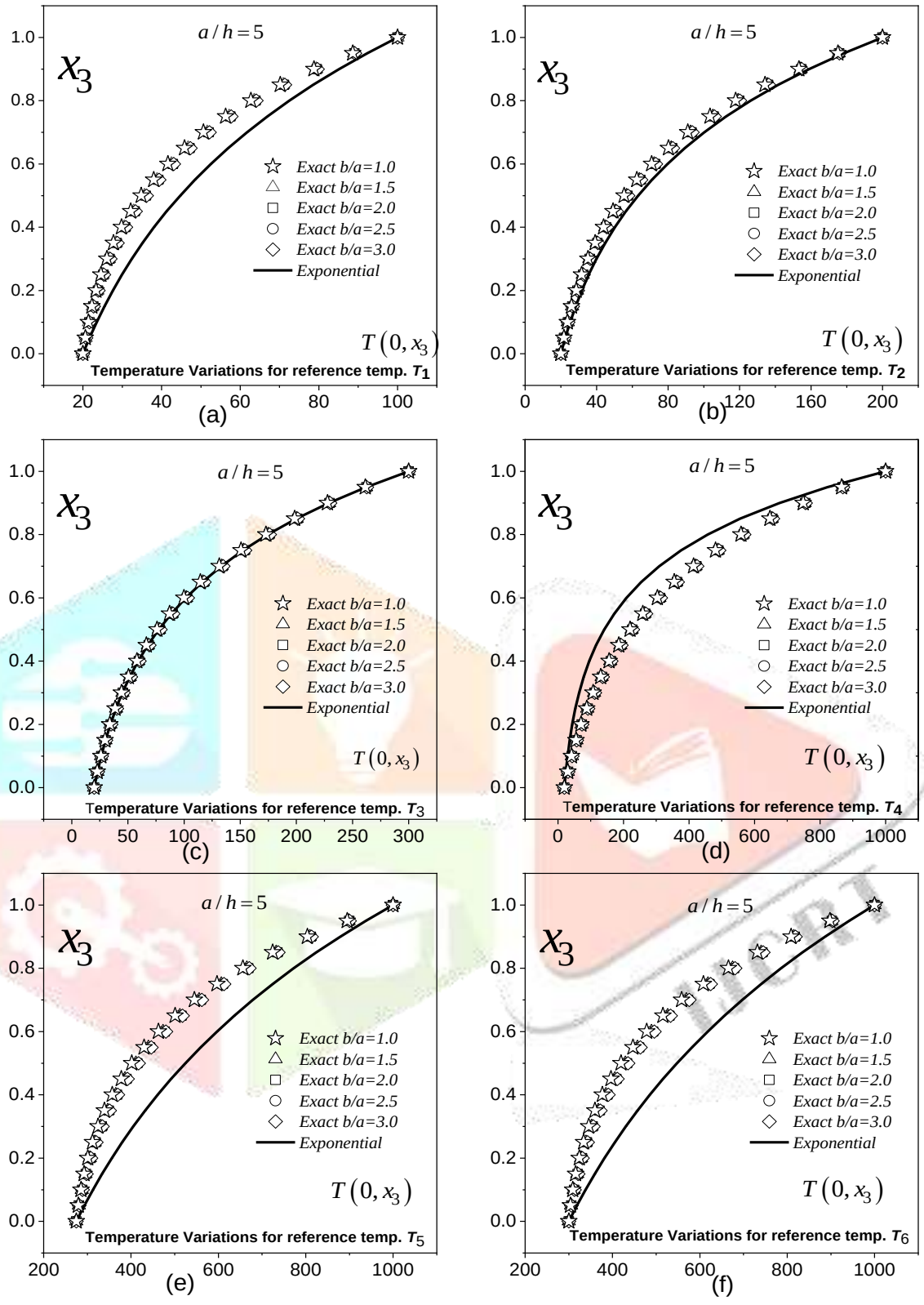

Fig. 8. Comparison of exact and exponential through thickness variation for various in-plane aspect ratios $\left(b/a\right)$ for FG plate (Material set 3)

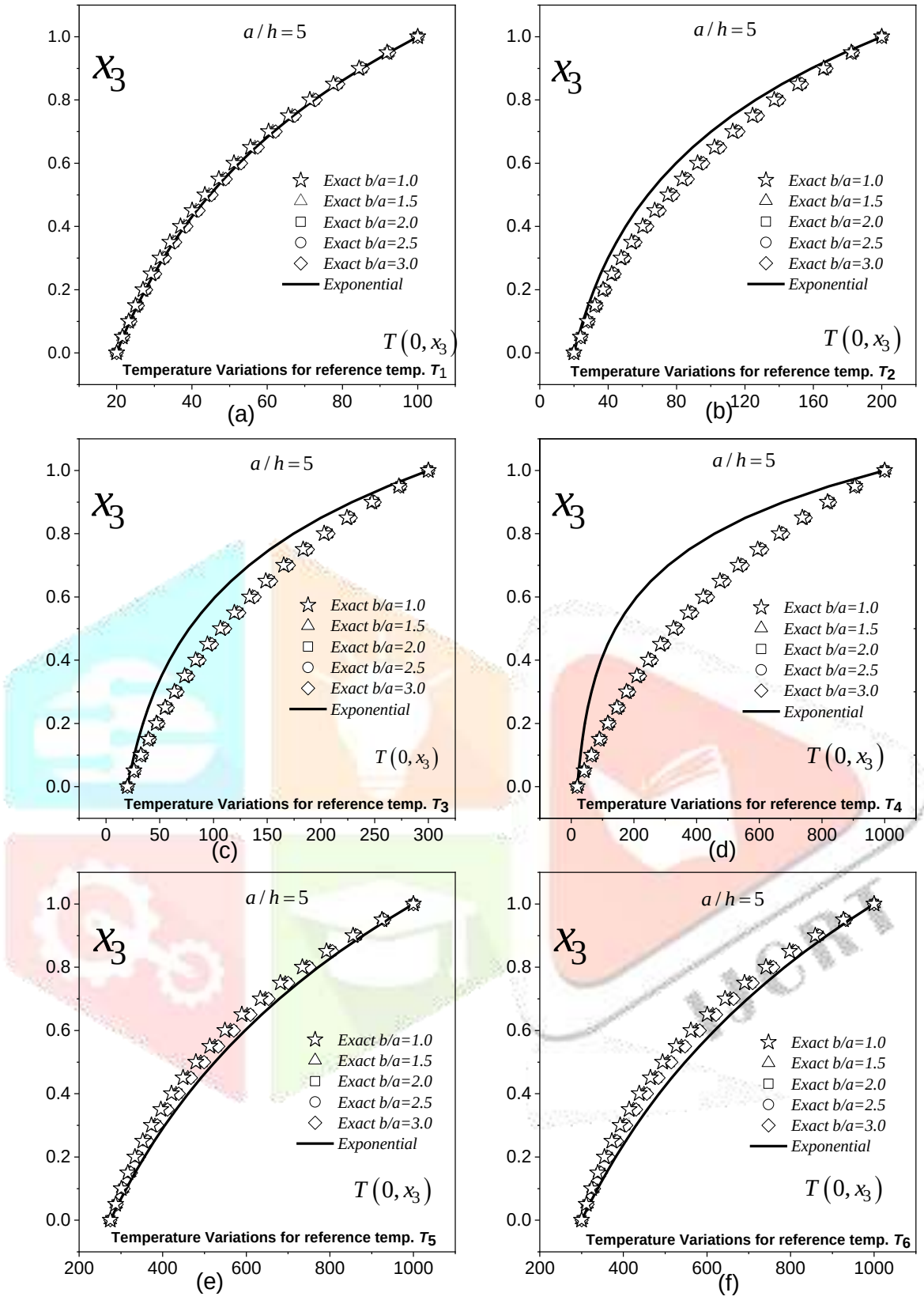

Fig. 9. Comparison of exact and exponential through thickness variation for various in-plane aspect ratios $\left(b/a\right)$ for FG plate (Material set 4)

Table 1. Conversion of Boundary Value Problem into Initial Value Problem's for thermal analysis

Integration Number	Down side edge $(x_{3bottom} = 0)$		Upper side edge $(x_{3top} = h)$	
	$T(x_3)$	$q_z(x_3)$	$T(x_3)$	$q_z(x_3)$
a)	Known	0 (considered)	M_{11}	M_{21}
b)	0 (considered)	1 (considered)	M_{12}	M_{22}
c) (Final)	$T(0)$ (known)	$K1$	$T(h)$ (considered)	$q_{x_3}(h)$

Table 2. Material Properties

Set	Material Properties				
1	At bottom, $z = 0 \Rightarrow$ Aluminium :	$E = 70\ GPa$	$\mu = 0.3$	λ=204 K^{-1}	α=23×10^{-6} $W_m^{-1}K^{-1}$
	At top, $z = h \Rightarrow$ Zirconia :	$E = 151\ GPa$	$\mu = 0.3$	λ=2.09 K^{-1}	α =10×10^{-6} $W_m^{-1}K^{-1}$
2	At bottom, $z = 0 \Rightarrow$ Aluminium :	$E = 70\ GPa$	$\mu = 0.3$	λ=204K^{-1}	α=23×10^{-6} $W_m^{-1}K^{-1}$
	At top, $z = h \Rightarrow$ Alumina :	$E = 380\ GPa$	$\mu = 0.326$	$\lambda = 10.40K^{-1}$	$\alpha = 7.4\times10^{-6}$ $W_m^{-1}K^{-1}$
3	At bottom, $z = 0 \Rightarrow$ Monel :	$E = 227.24\ GPa$	$\mu = 0.3$	λ=25 K^{-1}	α=15×10^{-6} $W_m^{-1}K^{-1}$
	At top, $z = h \Rightarrow$ Zirconia :	$E = 151\ GPa$	$\mu = 0.3$	λ=2.09 K^{-1}	α =10×10^{-6} $W_m^{-1}K^{-1}$
4	At bottom, $z = 0 \Rightarrow$ Aluminium :	$E = 70\ GPa$	$\mu = 0.3$	λ=233 K^{-1}	α=23.4×10^{-6} $W_m^{-1}K^{-1}$
	At top, $z = h \Rightarrow SiC$:	$E = 427\ GPa$	$\mu = 0.3$	λ=65 K^{-1}	$\alpha = 4.3\times10^{-6}$ $W_m^{-1}K^{-1}$

Ref. Kadoli et al. (2008) and Ji Ying et al. (2009)